



HAL
open science

Comparative analysis of neuroinvasion by Japanese encephalitis virulent and vaccine strains in an in cellulo model of human blood-brain barrier

Cécile Khou, Marco Aurelio Díaz-Salinas, Anaëlle da Costa, Christophe Préhaud, Patricia Jeannin, Philippe V. Afonso, Marco Vignuzzi, Monique Lafon, Nathalie Pardigon

► **To cite this version:**

Cécile Khou, Marco Aurelio Díaz-Salinas, Anaëlle da Costa, Christophe Préhaud, Patricia Jeannin, et al.. Comparative analysis of neuroinvasion by Japanese encephalitis virulent and vaccine strains in an in cellulo model of human blood-brain barrier. 2020. pasteur-02549123

HAL Id: pasteur-02549123

<https://pasteur.hal.science/pasteur-02549123>

Preprint submitted on 21 Apr 2020

HAL is a multi-disciplinary open access archive for the deposit and dissemination of scientific research documents, whether they are published or not. The documents may come from teaching and research institutions in France or abroad, or from public or private research centers.

L'archive ouverte pluridisciplinaire **HAL**, est destinée au dépôt et à la diffusion de documents scientifiques de niveau recherche, publiés ou non, émanant des établissements d'enseignement et de recherche français ou étrangers, des laboratoires publics ou privés.

1 **Comparative analysis of neuroinvasion by Japanese encephalitis virulent**
2 **and vaccine strains in an *in cellulo* model of human blood-brain barrier**

3
4
5 Cécile Khou^{1§#}, Marco Aurelio Díaz-Salinas^{1#}, Anaëlle da Costa^{2\$}, Christophe
6 Préhaud², Patricia Jeannin⁴, Philippe V. Afonso⁴, Marco Vignuzzi³, Monique
7 Lafon², Nathalie Pardigon^{1*}

8
9
10 ¹Unité de Recherche et d'Expertise Environnement et Risques Infectieux,
11 Groupe Arbovirus, Institut Pasteur, 25 Rue du Dr Roux, 75724 Paris, Cedex 15,
12 France.

13 ²Unité de Neuro-Immunologie Virale, Institut Pasteur, Paris, France.

14 ³Unité des Populations Virales et Pathogénèse, Institut Pasteur, Paris, France.

15 ⁴Unité d'Epidémiologie et Physiopathologie des Virus Oncogènes, Institut
16 Pasteur, CNRS UMR 3569, Paris, France.

17
18 [§]Current address: Direction Générale de l'Armement, Vert-le-Petit, France

19 ^{\$}Current address : TheraNexus, Fontenay-aux-Roses, France.

20
21 [#]These authors contributed equally to this work.

22
23 ^{*}Corresponding author

24 E-mail : pardigon@pasteur.fr

26

27 **ABSTRACT**

28 Japanese encephalitis virus (JEV) is the major cause of viral encephalitis
29 in South East Asia. It has been suggested that JEV gets access to the central
30 nervous system (CNS) as a consequence of a preceding inflammatory process
31 which leads to the blood-brain barrier (BBB) disruption and viral neuroinvasion.
32 However, what happens at early times of JEV contact with the BBB is poorly
33 understood. In the present work, we evaluated the ability of both a virulent and
34 a vaccine strain of JEV (JEV RP9 and SA14-14-2, respectively) to cross an *in*
35 *cellulo* human BBB model consisting of hCMEC/D3 human endothelial cells
36 cultivated on permeable inserts above SK-N-SH human neuroblastoma cells.
37 Using this system, we demonstrated that both JEV RP9 and SA14-14-2 are
38 able to cross the BBB without disrupting it at early times post-addition.
39 Furthermore, this BBB model was able to discriminate between the virulent RP9
40 and the vaccine SA14-14-2 strains, as demonstrated by the presence of almost
41 10 times more RP9 infectious particles that crossed the BBB than SA14-14-2
42 particles at a high MOI. Besides contributing to the understanding of early
43 events in JEV neuroinvasion, this *in cellulo* BBB model represents a suitable
44 and useful system to study the viral determinants of JEV neuroinvasiveness and
45 the molecular mechanisms by which this flavivirus crosses the BBB at early
46 times of neuroinvasion.

47

48

49

50

51

52 INTRODUCTION

53 *Flaviviruses* such as Japanese encephalitis virus (JEV) are arthropod-
54 borne viruses (arbovirus) that are transmitted through the bite of an infected
55 mosquito and may cause serious human diseases [1]. JEV is the main
56 causative agent of viral encephalitis in South East Asia, with an annual
57 incidence of around 68 000 cases [2]. About 30% of the cases are fatal, and
58 half of the survivors present neurological sequelae [3]. To date, no specific
59 treatment against JEV exists [3]. However, Japanese encephalitis is a
60 preventable disease as vaccines have been developed: the live-attenuated JEV
61 SA14-14-2 strain, as well as a recombinant vaccine and an inactivated one,
62 also based on the JEV SA14-14-2 strain [4, 5]. The live-attenuated vaccine was
63 obtained empirically after several passages of the JEV SA14 virulent strain in
64 primary hamster kidney cells [6]. Although highly efficient, cases of post-vaccine
65 encephalitis were also reported [7], suggesting that the vaccine strain JEV
66 SA14-14-2 is still neurovirulent in humans.

67 JEV has a positive-sense RNA genome encoding a single polyprotein
68 flanked by two untranslated regions (UTR) at its 5' and 3' ends. This polyprotein
69 is co- and post-translationally cleaved into three structural proteins (capsid C,
70 membrane prM and envelope E) involved in viral particle assembly and
71 antigenicity and seven non-structural proteins (NS1, NS2A, NS2B, NS3, NS4A,
72 NS4B and NS5) involved in genome replication, viral particle assembly and
73 evasion of innate immunity [1]. Due to an error-prone NS5 polymerase that
74 frequently introduces mutations in the viral genome during replication, a

75 *Flavivirus* population is not clonal, but rather a mix of multiple viral genomic
76 species (aka quasispecies) [8, 9].

77 JEV is a neuroinvasive and neurovirulent virus. It is associated with
78 neuroinflammation of the central nervous system (CNS) [10], and disruption of
79 the blood-brain barrier (BBB), as shown *in vivo* in murine and simian models
80 [10, 11]. Expression levels of tight junction proteins involved in maintaining BBB
81 functions such as occludin, claudin-5 and zonula occludens 1 (ZO-1) are
82 significantly decreased in symptomatic JEV-infected mice, suggesting physical
83 disruption of the BBB [11]. However, it seems that BBB disruption occurs after
84 infection of the CNS cells in a mouse model of JEV-induced encephalitis [11]
85 and that inflammatory response of infected astrocytes and pericytes plays a key
86 role in BBB leakage [11-13], suggesting that JEV can cross the BBB before
87 disrupting it. Indeed early studies of JEV infection of mouse brain demonstrated
88 that the virus was transported across the cerebral endothelium by endocytosis
89 [14]. Vesicular transport of cellular cargoes through endothelial cells is known
90 as transcytosis [15], but it is unclear whether this mechanism also applies to the
91 transport of JEV.

92 In contrast to virulent JEV strains as RP9, the vaccine strain SA14-14-2
93 was shown to be essentially non-neuroinvasive and non-neurovirulent in
94 weanling ICR mice, but is still highly neurovirulent in neonates [16]. JEV SA14-
95 14-2 genome displays 57 nucleotide differences positioned along the genome
96 when compared to the parental strain SA14, leading to 25 amino-acid
97 substitutions [16]. Mutations in the E protein seem to attenuate JEV
98 neurovirulence [17, 18], while mutations in the 5' UTR, capsid C and NS1-NS2A
99 protein coding regions have been found to attenuate JEV neuroinvasiveness in

100 a mouse model [18-20]. Despite the identification of these attenuating
101 mutations, the specific amino-acids contributing to the attenuation of JEV SA14-
102 14-2 are unknown.

103 Encephalitis incidents have occurred after vaccination with the SA14-14-
104 2 JEV strain, but no virus could be recovered from them [7]. Whether these
105 neurological adverse events originated from virus reversion to a virulent
106 phenotype, a specific viral neuroinvasive and neurovirulent sub-population or
107 from host determinants is still unknown [7]. In any case, the JEV vaccine strain,
108 although much less neurovirulent and neuroinvasive than its parental
109 counterpart, must have crossed the BBB in order to reach the CNS and initiate
110 encephalitis.

111 The BBB is the physical and physiological barrier between the brain and
112 the blood compartments in vertebrates, and it is comprised of a network of
113 different cell types including the brain microvascular endothelium along with
114 pericytes, astrocytes, microglia and the basement membrane [21]. Many BBB
115 models have been developed in order to facilitate studies on the biology and
116 pathophysiology of its diverse components, as well as to evaluate drug
117 transport to the brain [22]. The brain microvascular endothelial cell line
118 hCMEC/D3 exhibits a stable growth and endothelial marker characteristics that
119 makes it suitable to form a reproducible and easy-to-grow BBB *in cellulo*.
120 hCMEC/D3 monolayer displays good restricted permeability to paracellular
121 tracers and retains most of the transporters and receptors present on *in vivo*
122 BBB [23]. Accordingly, hCMEC/D3 cells have been used to investigate host-
123 pathogen interactions with human pathogens that affect the CNS [24, 25].

124 In the present study, we evaluated the ability of both a virulent and a
125 vaccine strain of JEV (JEV RP9 and SA14-14-2, respectively) to cross an *in*
126 *cellulo* human BBB model consisting of hCMEC/D3 human endothelial cells
127 cultivated on permeable supports above SK-N-SH human neuroblastoma cells.
128 Using this system, we demonstrated that both JEV RP9 and SA14-14-2 strains
129 are able to cross the BBB without disrupting it at early times post-addition. More
130 importantly this BBB model is discriminant as about 10 times more RP9 than
131 SA14-14 infectious particles may cross the barrier at a high MOI. Besides
132 contributing to the understanding of early events in JEV neuroinvasion, this *in*
133 *cellulo* BBB model represents a useful tool to examine the viral determinants of
134 JEV neuroinvasiveness and the molecular mechanisms by which this flavivirus
135 cross the BBB.

136

137 **MATERIAL AND METHODS**

138 **Cell lines and JEV strains**

139 Human endothelial cells hCMEC/D3 [23], were maintained at 37°C on rat
140 collagen diluted at 100µg/mL in water (Cultrex; catalog no. 3443-100-01) in
141 EndoGro medium (Merck Millipore; catalog no. SCME004) supplemented with
142 5% fetal bovine serum (FBS) and 10mM HEPES buffer (Sigma-Aldrich; catalog
143 no. 83264). hCMEC/D3 cells can form tight junctions when cultured for 6 days
144 at 37°C. Human neuroblastoma cells SK-N-SH (ATCC HTB-11) were
145 maintained at 37°C in Dulbecco modified Eagle medium (DMEM) supplemented
146 with 10% heat-inactivated FBS. *Cercopithecus aethiops* monkey kidney Vero
147 cells were maintained at 37°C in DMEM supplemented with 5% heat-inactivated

148 FBS. *Aedes albopictus* mosquito cells C6/36 were maintained at 28°C in
149 Leibovitz medium (L15) supplemented with 10% heat-inactivated FBS.
150 A molecular cDNA clone of JEV genotype 3 strain RP9 was kindly provided by
151 Dr. Yi-Ling Lin [26]. This plasmid was modified in our laboratory as previously
152 described [27]. To produce infectious virus, the molecular clone
153 (pBR322(CMV)-JEV-RP9) was transfected into C6/36 cells using Lipofectamine
154 2000 (Life Technologies; catalog no. 11668-019). Once a cytopathic effect was
155 visible, viral supernatant was collected and used to infect C6/36 cells. As
156 hCMEC/D3 monolayer is very sensitive to any change of medium, we used
157 viruses produced from cells grown in the same medium as the one used to grow
158 endothelial cells (EndoGro medium). A CD.JEVAX® (JEV SA14-14-2) vaccine
159 vial was kindly provided by Dr. Philippe Dussart (Institut Pasteur of Phnom
160 Penh, Cambodia). The vaccine was reconstituted with 500µL of DMEM. 250µL
161 of reconstituted vaccine were used to infect Vero cells for 7 days. Viral
162 supernatants were collected and used to infect C6/36 cells cultivated in
163 EndoGro medium supplemented with 2% FBS. Both JEV RP9 and SA14-14-2
164 viral supernatant stocks were collected 3 days after infection and the infectious
165 titer was determined in Vero cells through a focus-forming assay (see below).

166 **Antibodies**

167 Mouse hybridomas producing the monoclonal antibody 4G2 anti-
168 *Flavivirus* E protein were purchased from the ATCC (catalog no. HB-112), and a
169 highly-purified antibody preparation was produced by RD Biotech (Besançon,
170 France). Mouse monoclonal antibody anti-JEV NS5 was kindly provided by Dr.
171 Yoshiharu Matsura [28]. Horseradish peroxidase (HRP)-conjugated goat anti-
172 mouse IgG antibody was obtained from Bio-Rad Laboratories (catalog no. 170-

173 6516). Alexa Fluor 488-conjugated goat anti-mouse IgG antibody was obtained
174 from Jackson ImmunoResearch (catalog no. 115-545-003).

175 **Evaluation of JEV neuroinvasive capacity**

176 $5 \cdot 10^4$ hCMEC/D3 cells were seeded on 12-well Transwell[®] permeable
177 inserts (Corning; catalog no. 3460) in EndoGro medium supplemented with 5%
178 FBS for 5 days. $2 \cdot 10^5$ SK-N-SH cells were seeded in 12-well tissue culture
179 plates in EndoGro supplemented with 2% FBS. Permeable inserts containing
180 hCMEC/D3 cells were then transferred in these culture plates and medium was
181 replaced by EndoGro medium supplemented with 2% FBS. Aliquots of virus
182 were diluted the next day in 50 μ L of EndoGro medium supplemented with 2%
183 FBS, heated at 37°C and then added to the cells. Cells were incubated at 37°C
184 until collection.

185 **Focus-forming assay (FFA)**

186 Vero cells were seeded in 24-well plates. Ten-fold dilutions of virus
187 samples were prepared in DMEM and 200 μ L of each dilution was added to the
188 cells. The plates were incubated for 1h at 37°C. Unabsorbed virus was removed
189 and 800 μ L of DMEM supplemented with 0.8% carboxymethyl cellulose (CMC),
190 5 mM HEPES buffer, 36 mM sodium bicarbonate, and 2% FBS were added to
191 each well, followed by incubation at 37°C for 48h for JEV RP9 or for 72h for
192 JEV SA14-14-2. The CMC overlay was aspirated, and the cells were washed
193 with PBS and fixed with 4% paraformaldehyde for 20 min, followed by
194 permeabilization with 0.1% Triton X-100 for 5 min. After permeabilization, the
195 cells were washed with PBS and incubated for 1h at room temperature with
196 anti-E antibody (4G2), followed by incubation with HRP-conjugated anti-mouse
197 IgG antibody. The assays were developed with the Vector VIP peroxidase

198 substrate kit (Vector Laboratories; catalog no. SK-4600) according to the
199 manufacturer's instructions. The viral titers were expressed in focus-forming
200 units (FFU) per milliliter.

201 **Lucifer Yellow (LY) permeability assays**

202 LY dye migration through the BBB monolayers was performed as
203 previously described [24]. Briefly, Transwell® inserts containing hCMEC/D3
204 monolayers were transferred in culture wells containing 1.5 mL of Hanks'
205 Buffered Salt Solution (HBSS) supplemented with 10 mM of HEPES buffer, 1
206 mM of sodium pyruvate and 50µM of LY (Sigma-Aldrich; catalog no. L0144).
207 The culture medium inside the Transwell® inserts was replaced with 500µL of
208 HBSS buffer. Cells were incubated at 37°C for 10 min. Permeable inserts were
209 then transferred in culture well containing 1.5 mL of HBSS buffer and incubated
210 at 37°C for 15 min. They were then transferred in culture well containing 1.5 mL
211 of HBSS buffer and incubated at 37°C for 20 min. Concentrations of LY in the
212 wells were determined using a fluorescent spectrophotometer (Berthold,
213 TriStar² LB 942). The emission at 535 nm was measured with an excitation light
214 at 485 nm. The endothelial permeability coefficient of LY was calculated in
215 centimeters/min (cm/min), as previously described [29].

216 **Virus infections**

217 10^5 hCMEC/D3 cells were seeded on coverslips in 24-well tissue culture
218 plates in EndoGro medium supplemented with 5% FBS. After 5 days, cell
219 medium was replaced with 1 mL of EndoGro medium supplemented with 2%
220 FBS. 10^5 SK-N-SH cells were seeded on coverslips in 24-well tissue culture
221 plates in DMEM supplemented with 2% FBS. Aliquots of virus were diluted in
222 200µL of medium and added to the cells. Plates were incubated for 1h at 37°C.

223 Unabsorbed virus was removed and 1mL of EndoGro or DMEM supplemented
224 with 2% FBS was added to the cells, followed by incubation at 37°C until
225 collection.

226 **Immunofluorescence analysis (IFA)**

227 All the following steps were performed at room temperature. Cells were
228 fixed with 4% paraformaldehyde for 20 min followed by permeabilization with
229 0.1% Triton X-100 for 5 min. After permeabilization, the cells were washed with
230 PBS and incubated for 5 min with PBS containing 1% BSA. The cells were then
231 washed with PBS and incubated for 1h with anti-JEV NS5 antibody diluted at
232 1:200 in PBS, followed by incubation with Alexa Fluor 488-conjugated anti-
233 mouse IgG antibody diluted at 1:500 in PBS. The coverslips were mounted with
234 ProLong gold antifade reagent with DAPI (Life Technologies; catalog no.
235 P36931). The slides were examined using a fluorescence microscope (EVOS
236 FL Cell Imaging System).

237 **Gene expression studies**

238 $5 \cdot 10^4$ hCMEC/D3 cells were seeded on 12-well Transwell® insert filters
239 in EndoGro medium supplemented with 5% FBS for 5 days. $2 \cdot 10^5$ SK-N-SH
240 cells were seeded in 12-well tissue culture plates in EndoGro supplemented
241 with 2% FBS. Transwell® containing hCMEC/D3 cells were then transferred in
242 these culture plates and medium was replaced by EndoGro medium
243 supplemented with 2% FBS. Cells were incubated at 37°C. At 24h post-contact,
244 total RNA of hCMEC/D3 cells were extracted using NucleoSpin RNA kit
245 (Macherey-Nagel; catalog no. 740955.50) following the manufacturer's
246 instructions. 200 ng of total RNA were used to produce cDNA using the
247 SuperScript II Reverse Transcriptase (Thermo Fisher; catalog no. 18064014)

248 according to the manufacturer's instructions. Quantitative PCR were performed
249 on 2µL of cDNA using SYBR Green PCR Master Mix (Thermo Fisher; catalog
250 no. 4309155) according to the manufacturer's instructions. The CFX96 real-time
251 PCR system (Bio-Rad) was used to measure SYBR green fluorescence with the
252 following program: an initial PCR activation at 95°C (10 min), 40 cycles of
253 denaturation at 95°C (15s) and annealing-extension at 60°C (1 min). Results
254 were analyzed using the CFX Manager Software (Bio-Rad) gene expression
255 analysis tool. GAPDH was used as the reference gene. Primers used in gene
256 expression studies are listed in Table 1.

257 **Quantification of JEV RNA copies number**

258 Total RNA from JEV BBB-crossing samples was extracted using
259 NucleoSpin®RNA kit (Macherey-Nagel; 740955.50) according to the
260 manufacturer's instructions. The number of JEV RNA copies present in BBB-
261 crossing samples was determined by RT-qPCR using TaqMan® Fast Virus 1-
262 Step Master Mix kit (Applied Biosystems®, 4444432) according to the
263 manufacturer's instructions. The forward and reverse primers (Sigma-Aldrich®)
264 were 5'GAAGATGTCAACCTAGGGAGC3' and
265 5'TGGCGAATTCTTCTTTAAGC3' respectively, while
266 [6FAM]AAGAGCCGTGGGAAAGGGAGA[BHQ1] was the probe for the assay.
267 JEV RNA copies were calculated from a standard curve generated by
268 amplifying known amounts of *in vitro*-transcribed RP9 NS5 gene region cloned
269 and under SP6 promotor control. The *in vitro* transcription was performed using
270 mMESAGE mMACHINE™ SP6 kit (Invitrogen, Thermo Fisher Scientific,
271 AM1340) following the manufacturer's instructions.

272 **Statistical analysis**

273 Unpaired two-tailed *t* test, Mann-Whitney test and ANOVA test corrected
274 with Tukey method for multiple comparisons were used to compare
275 experimental data. GraphPad Prism 7 was used for these statistical analyses.

276

277 **RESULTS**

278 **hCMEC/D3 cell monolayers grown on permeable inserts form a BBB**

279 **whose properties are not affected by SK-N-SH cells presence.** A basic *in*

280 *cellulo* model to study JEV neuroinvasion should consist of two main

281 components: 1) a cell monolayer mimicking the BBB, and 2) a brain tissue-

282 derived cell line permissive to JEV. Based on our previous work [24], we chose

283 to use hCMEC/D3 human endothelial cells monolayers cultivated on permeable

284 inserts and place these inserts in wells in which human neuroblastoma SK-N-

285 SH cells were grown, in order to partly mimic the brain parenchyma. Relevant

286 parameters of a functional BBB model, such as permeability and presence of

287 cell transporters and receptors specific of hCMEC/D3 cells were evaluated

288 when the endothelial cells were or not grown above SK-N-SH monolayers (Fig.

289 1). Permeability measurement of hCMEC/D3 monolayers through evaluation of

290 Lucifer Yellow (LY) passage showed no significant difference whether SK-N-SH

291 cells were present or not (Fig. 1A, + or - respectively). Moreover, the relative

292 RNA level of genes coding for proteins involved both in cell receptors (Fig. 1B)

293 and transporters (Fig. 1C) characteristic of endothelial barriers were similar in

294 the two conditions, suggesting that the culture of neuroblastoma cells under the

295 inserts on which hCMEC/D3 were grown did not disturb the endothelial cell

296 intrinsic BBB properties and actually makes of this *in cellulo* BBB model a useful

297 tool to study the neuroinvasion ability of JEV.

298

299 **JEV SA14-14-2 is less replicative than JEV RP9 in SK-N-SH cells.**

300 Neuroblastoma SK-N-SH cells are susceptible to both the virulent JEV RP9
301 strain and the SA14-14-2 attenuated strain [27, 30]. However, a direct
302 comparison between replication of these two JEV strains in that cell line has not
303 been described. We thus evaluated replication of each JEV strain in SK-N-SH
304 cells at 24 and 48 hpi (Fig. 2). As expected, both JEV strains infected the
305 neuroblastoma-derived cell line as demonstrated by the detection of a viral
306 antigen (NS5 protein) through immunofluorescence assays (Fig. 2A). However,
307 the viral progeny of JEV SA14-14-2 vaccine strain produced in SK-N-SH cells at
308 24 and 48 hpi was significantly lower than that of JEV RP9 (1.7 and 1.2 log₁₀
309 less at 24 and 48 hpi respectively, Fig. 2B), suggesting that JEV SA14-14-2 is
310 less neurovirulent than JEV RP9 in human cell cultures.

311

312 **Neither JEV RP9 nor JEV SA14-14-2 infects hCMEC/D3 cells after they**

313 **form a BBB.** In order to examine the susceptibility of our hCMEC/D3 BBB
314 model to JEV infection, the cells were grown 6 days on coverslips to allow the
315 BBB to form, then inoculated with either RP9 or SA14-14-2 JEV strain (Fig. 3).
316 The presence of the NS5 viral protein as infection evidence was assessed by
317 immunofluorescence microscopy as described in the Material and Methods
318 section. No fluorescence signal was observed in hCMEC/D3 BBB-forming
319 monolayer either at 24 or 48 hpi (Fig. 3A). Surprisingly, hCMEC/D3 cells could
320 be infected by either JEV strains when they were inoculated after only one day
321 of culture (ie not forming of a BBB), as detected through the same
322 immunofluorescence approach (Fig. 3B). Moreover, in this condition, both JEV

323 strains produced infectious viral progeny in hCMEC/D3, although the RP9 viral
324 titer was significant higher by around 2 log than that observed for SA14-14-2
325 (Fig. 3C). These results suggest that hCMEC/D3 cells are not susceptible to
326 JEV infection when they already have formed a barrier, but they are JEV
327 permissive before tight junctions formation.

328

329 **Neither JEV RP9 nor JEV SA14-14-2 disrupts the BBB when added for 6h.**

330 It has been suggested that JEV infects brain tissue cells as a consequence of a
331 preceding inflammatory process which leads to the BBB disruption and viral
332 neuroinvasion [31, 32]. However, the very early events of JEV BBB crossing are
333 still poorly understood. In order to evaluate the neuroinvasive ability of JEV in
334 our BBB model at early times post-addition, hCMEC/D3 cells cultivated on
335 permeable inserts to form a BBB above SK-N-SH cells monolayer were
336 exposed to either JEV RP9 or SA14-14-2 virus addition (MOI=1 or 10; Fig. 4).
337 The permeability of the BBB at 6 hpi in the presence of the 2 different JEV
338 strains did not show a significant difference when compared to that of the mock-
339 infected condition (Fig. 4A), suggesting that the BBB model was not disturbed
340 either by the JEV strains or the MOIs used.

341

342 **More JEV RP9 infectious particles may cross the *in cellulo* BBB model**
343 **than JEV SA14-14-2.**

344 Since the BBB permeability was not affected by the addition of either virus, we
345 examined the viral crossing of each strain by evaluating the quantity of viral
346 RNA and infectious particles in the supernatants under the inserts (Fig. 4B and
347 C). The number of viral RNA copies detected for both viruses was 1.7 log₁₀

348 higher when a MOI of 10 was used in comparison to a MOI of 1 (Fig. 4B),
349 suggesting that the higher the JEV viral load, the greater the number of viral
350 particles crossing the BBB. Of note, there was no significant difference in the
351 viral RNA copy number between the JEV strains for each MOI (MOI=1 or =10,
352 Fig. 4B). However, the infectious titers of the JEV particles that crossed the
353 BBB was surprisingly different between the RP9 and SA14-14-2 strains, as
354 about 3 times more RP9 infectious particles were found in the supernatants
355 under the inserts than SA14-14-2 when an MOI of 1 was used, and close to 10
356 times for a MOI of 10 (Fig. 4C). Calculation of the specific infectivity for JEV
357 RP9 and SA14-14-2 strains as the ratio between the detected JEV RNA copy
358 number per infectious focus-forming unit did not show a significant difference
359 between the 2 viral stocks (Fig. 5A). Interestingly, the specific infectivity for the
360 RP9 BBB-crossing samples was significantly lower than that observed for the
361 vaccine strain SA14-14-2 with a 3 to 10 fold decrease for MOI=1 and =10
362 respectively (Fig. 5B). These results indicate that more JEV RP9 infectious
363 particles may cross our BBB model than SA14-14, and demonstrate that this *in*
364 *cellulo* barrier is capable of discriminating between 2 viruses with different
365 neuroinvasive capabilities.

366

367 **DISCUSSION**

368 Several lines of research in either *in vivo* and *in vitro* systems have
369 suggested that JEV infects brain tissue cells as a consequence of a preceding
370 inflammatory process which would lead to the BBB disruption and viral
371 neuroinvasion [31, 32]. While *in vivo* approaches are useful to understand the
372 systemic viral disease, *in vitro* models are also useful because they allow

373 studying the molecular mechanisms that govern viral pathogenesis. In this
374 regard, previous approaches have been used to characterize JEV
375 neuroinvasion properties at late times of infection, mainly 24 hpi or later [30, 33-
376 35]. However, knowledge relative to the early times of JEV contact with the BBB
377 is poor, if not null.

378 In this study, we have used an *in cellulo* model of a human BBB to
379 compare JEV RP9 virulent and JEV SA14-14-2 vaccine strain ability to cross
380 the BBB at early times post-addition. We have shown that both JEV RP9 and
381 SA14-14-2 are able to cross the BBB without disrupting it at 6 hpi (Fig. 4). This
382 finding is very relevant because it suggests that JEV could be able to get
383 access to the CNS and establish a primary infection there without the preceding
384 need of inflammatory cytokines that could lead to BBB disruption prior CNS
385 cells viral infection as it is currently thought [31, 32].

386 Moreover, the fact that both JEV RP9 and SA14-14-2 strains crossed the
387 BBB without infecting its endothelial cells, nor disrupting the barrier, also
388 suggests that JEV is able to cross the BBB in a transcellular way through the
389 endothelial cells or in a paracellular way between the endothelial cells. These
390 observations are consistent with other studies conducted *in vivo* in mice and
391 monkeys [11, 16, 36]. Observations of JEV-infected suckling mice brain by
392 electron-microscopy suggested that JEV crosses the BBB endothelial cells by
393 transcytosis [14]. Regardless of these observations, currently there is no
394 published data to support this hypothesis from biochemical, genetics or
395 functional approaches. The combination of these approaches, together with the
396 use of our *in cellulo* BBB model and JEV strains with different neuroinvasive

397 capabilities such as the ones used in this work would be useful to identify which
398 cell mechanisms are "highjacked" by these pathogens to cross the BBB.

399 Interestingly, our specific infectivity data suggest that JEV RP9 infectious
400 particles crossed the BBB more efficiently than JEV SA14-14-2 (Fig. 5).
401 Comparison of the transcriptome from hCMEC/D3 cells forming a BBB to which
402 either JEV RP9, SA14-14-2 or no virus was added for 6h showed no significant
403 difference in the levels of gene expression (fold-change threshold of 2, data not
404 shown). This suggests that an early cell response is not responsible for the
405 differential BBB crossing of JEV RP9 versus JEV SA-14-14-2 particles we
406 observed (Fig. 4C), and that it most likely stems from viral factors. It is also
407 possible that the difference in the JEV RP9 and SA14-14-2 infectious particles
408 ability to cross the *in cellulo* BBB relies on specific protein interactions, for
409 example, interaction of the viral particle with a strain-specific cell surface
410 receptor for viral entry. A full characterization of the viral particles that are able
411 to cross the BBB including by deep-sequencing of their RNA content and
412 examining the endothelial cells forming the BBB after contact with either virus
413 by electron microscopy, together with uncovering specific cell receptor(s) for
414 JEV strains could help solving these issues.

415 Surprisingly, we found that hCMEC/D3 were permissive to both RP9 and
416 SA14-14-2 strains only when the BBB formation was not completed (Fig. 3B),
417 suggesting that formation of tight junctions between these cells could make the
418 JEV cell entry receptor(s) inaccessible to the virus. Based on our data and
419 considering the current model of JEV neuroinvasion that suggests disruption of
420 the BBB following CNS viral infection [11], endothelial cells from a disrupted
421 barrier might become permissive to JEV because of better accessibility to cell

422 entry receptor(s), and these cells, upon infection, could in turn become a new
423 source of viral production contributing to JEV infection of the CNS.

424 In conclusion, our study demonstrates that both JEV RP9 and SA14-14-2
425 are able to cross a BBB model without disrupting it at early times post-addition
426 and that the BBB formed by human endothelial cells represents a useful
427 discriminant *in cellulo* model to characterize viral determinants of JEV
428 neuroinvasiveness as well as a tool to study the molecular mechanisms by
429 which these pathogens cross the BBB.

430

431 **ACKNOWLEDGMENTS**

432 Transcriptomic analysis was performed by the Pôle Biomixs of the Institut
433 Pasteur Center for Technological Resources and Research (C2RT). We thank
434 Dr. Philippe Dussart for providing the JEV SA14-14-2 vaccine, Dr. Yi-Lin Ling
435 for providing the JEV-RP9 cDNA clone and Dr. Yoshiharu Matsuura for
436 providing the anti-JEV NS5 antibody. This work was supported by a grant from
437 the Seventh Framework Program (FP7) under grant number 278433-
438 PREDEMICS. CK was funded by the French Ministry of Defense / Délégation
439 Générale de l'Armement. MAD-S was funded by the DARPA INTERCEPT
440 program (DARPA cooperative agreement #HR0011-17-2-0023. Please note
441 that the content of the article does not necessarily reflect the position or the
442 policy of the U.S. government and no official endorsement should be inferred).

443

444 **REFERENCES**

- 445 1. Lindenbach BD, T.H., Rice CM., *Flaviviridae: The viruses and their*
446 *replication*. Fields Virology, 5th ed. Philadelphia, PA. Lippincot-Raven
447 Publishers., 2007: p. 1101-1152.
- 448 2. Campbell, G.L., et al., *Estimated global incidence of Japanese*
449 *encephalitis: a systematic review*. Bull World Health Organ, 2011. **89**(10):
450 p. 766-74, 774A-774E.
- 451 3. Solomon, T., et al., *Japanese encephalitis*. J Neurol Neurosurg
452 Psychiatry, 2000. **68**(4): p. 405-15.
- 453 4. Yun, S.I. and Y.M. Lee, *Japanese encephalitis: the virus and vaccines*.
454 Hum Vaccin Immunother, 2014. **10**(2): p. 263-79.
- 455 5. Chambers, T.J., et al., *Yellow fever/Japanese encephalitis chimeric*
456 *viruses: construction and biological properties*. J Virol, 1999. **73**(4): p.
457 3095-101.
- 458 6. Eckels, K.H., et al., *Japanese encephalitis virus live-attenuated vaccine,*
459 *Chinese strain SA14-14-2; adaptation to primary canine kidney cell*
460 *cultures and preparation of a vaccine for human use*. Vaccine, 1988.
461 **6**(6): p. 513-8.
- 462 7. Liu, Y., et al., *Safety of Japanese encephalitis live attenuated vaccination*
463 *in post-marketing surveillance in Guangdong, China, 2005-2012*.
464 Vaccine, 2014. **32**(15): p. 1768-73.
- 465 8. Eigen, M., *Viral quasispecies*. Sci Am, 1993. **269**(1): p. 42-9.
- 466 9. Domingo, E., J. Sheldon, and C. Perales, *Viral quasispecies evolution*.
467 Microbiol Mol Biol Rev, 2012. **76**(2): p. 159-216.
- 468 10. Myint, K.S., et al., *Neuropathogenesis of Japanese encephalitis in a*
469 *primate model*. PLoS Negl Trop Dis, 2014. **8**(8): p. e2980.

- 470 11. Li, F., et al., *Viral Infection of the Central Nervous System and*
471 *Neuroinflammation Precede Blood-Brain Barrier Disruption during*
472 *Japanese Encephalitis Virus Infection*. J Virol, 2015. **89**(10): p. 5602-14.
- 473 12. Chang, C.Y., et al., *Disruption of in vitro endothelial barrier integrity by*
474 *Japanese encephalitis virus-Infected astrocytes*. Glia, 2015. **63**(11): p.
475 1915-1932.
- 476 13. Chen, C.J., et al., *Infection of pericytes in vitro by Japanese encephalitis*
477 *virus disrupts the integrity of the endothelial barrier*. J Virol, 2014. **88**(2):
478 p. 1150-61.
- 479 14. Liou, M.L. and C.Y. Hsu, *Japanese encephalitis virus is transported*
480 *across the cerebral blood vessels by endocytosis in mouse brain*. Cell
481 Tissue Res, 1998. **293**(3): p. 389-94.
- 482 15. Tuma, P. and A.L. Hubbard, *Transcytosis: crossing cellular barriers*.
483 Physiol Rev, 2003. **83**(3): p. 871-932.
- 484 16. Yun, S.I., et al., *Comparison of the live-attenuated Japanese encephalitis*
485 *vaccine SA14-14-2 strain with its pre-attenuated virulent parent SA14*
486 *strain: similarities and differences in vitro and in vivo*. J Gen Virol, 2016.
487 **97**(10): p. 2575-2591.
- 488 17. Yun, S.I., et al., *A molecularly cloned, live-attenuated japanese*
489 *encephalitis vaccine SA14-14-2 virus: a conserved single amino acid in*
490 *the ij Hairpin of the Viral E glycoprotein determines neurovirulence in*
491 *mice*. PLoS Pathog, 2014. **10**(7): p. e1004290.
- 492 18. Gromowski, G.D., C.Y. Firestone, and S.S. Whitehead, *Genetic*
493 *Determinants of Japanese Encephalitis Virus Vaccine Strain SA14-14-2*

- 494 *That Govern Attenuation of Virulence in Mice*. J Virol, 2015. **89**(12): p.
495 6328-37.
- 496 19. Melian, E.B., et al., *NS1' of flaviviruses in the Japanese encephalitis virus*
497 *serogroup is a product of ribosomal frameshifting and plays a role in viral*
498 *neuroinvasiveness*. J Virol, 2010. **84**(3): p. 1641-7.
- 499 20. Ye, Q., et al., *A single nucleotide mutation in NS2A of Japanese*
500 *encephalitis-live vaccine virus (SA14-14-2) ablates NS1' formation and*
501 *contributes to attenuation*. J Gen Virol, 2012. **93**(Pt 9): p. 1959-64.
- 502 21. Abbott, N.J., *Blood-brain barrier structure and function and the*
503 *challenges for CNS drug delivery*. J Inherit Metab Dis, 2013. **36**(3): p.
504 437-49.
- 505 22. Helms, H.C., et al., *In vitro models of the blood-brain barrier: An overview*
506 *of commonly used brain endothelial cell culture models and guidelines*
507 *for their use*. J Cereb Blood Flow Metab, 2016. **36**(5): p. 862-90.
- 508 23. Weksler, B., I.A. Romero, and P.O. Couraud, *The hCMEC/D3 cell line as*
509 *a model of the human blood brain barrier*. Fluids Barriers CNS, 2013.
510 **10**(1): p. 16.
- 511 24. da Costa, A., et al., *Innovative in cellulo method as an alternative to in*
512 *vivo neurovirulence test for the characterization and quality control of*
513 *human live Yellow Fever virus vaccines: A pilot study*. Biologicals, 2018.
514 **53**: p. 19-29.
- 515 25. da Costa, A., et al., *A Human Blood-Brain Interface Model to Study*
516 *Barrier Crossings by Pathogens or Medicines and Their Interactions with*
517 *the Brain*. J Vis Exp, 2019(146).

- 518 26. Liang, J.J., et al., *A Japanese encephalitis virus vaccine candidate strain*
519 *is attenuated by decreasing its interferon antagonistic ability.* Vaccine,
520 2009. **27**(21): p. 2746-54.
- 521 27. de Wispelaere, M., M.P. Frenkiel, and P. Despres, *A Japanese*
522 *encephalitis virus genotype 5 molecular clone is highly neuropathogenic*
523 *in a mouse model: impact of the structural protein region on virulence.* J
524 Virol, 2015. **89**(11): p. 5862-75.
- 525 28. Katoh, H., et al., *Heterogeneous nuclear ribonucleoprotein A2*
526 *participates in the replication of Japanese encephalitis virus through an*
527 *interaction with viral proteins and RNA.* J Virol, 2011. **85**(21): p. 10976-
528 88.
- 529 29. Siflinger-Birnboim, A., et al., *Molecular sieving characteristics of the*
530 *cultured endothelial monolayer.* J Cell Physiol, 1987. **132**(1): p. 111-7.
- 531 30. Hsieh, J.T., et al., *Japanese encephalitis virus neuropenetrance is driven*
532 *by mast cell chymase.* Nat Commun, 2019. **10**(1): p. 706.
- 533 31. Turtle, L. and T. Solomon, *Japanese encephalitis - the prospects for new*
534 *treatments.* Nat Rev Neurol, 2018. **14**(5): p. 298-313.
- 535 32. Mustafa, Y.M., et al., *Pathways Exploited by Flaviviruses to Counteract*
536 *the Blood-Brain Barrier and Invade the Central Nervous System.* Front
537 Microbiol, 2019. **10**: p. 525.
- 538 33. Liu, T.H., et al., *The blood-brain barrier in the cerebrum is the initial site*
539 *for the Japanese encephalitis virus entering the central nervous system.*
540 J Neurovirol, 2008. **14**(6): p. 514-21.

- 541 34. Agrawal, T., et al., *Japanese encephalitis virus disrupts cell-cell junctions*
542 *and affects the epithelial permeability barrier functions*. Plos One, 2013.
543 **8**(7): p. e69465.
- 544 35. Wang, K., et al., *IP-10 Promotes Blood-Brain Barrier Damage by*
545 *Inducing Tumor Necrosis Factor Alpha Production in Japanese*
546 *Encephalitis*. Front Immunol, 2018. **9**: p. 1148.
- 547 36. Lai, C.Y., et al., *Endothelial Japanese encephalitis virus infection*
548 *enhances migration and adhesion of leukocytes to brain microvascular*
549 *endothelia via MEK-dependent expression of ICAM1 and the CINC and*
550 *RANTES chemokines*. J Neurochem, 2012. **123**(2): p. 250-61.
- 551 37. Cecchelli, R., et al., *A stable and reproducible human blood-brain barrier*
552 *model derived from hematopoietic stem cells*. Plos One, 2014. **9**(6): p.
553 e99733.
- 554 38. Lippmann, E.S., et al., *Derivation of blood-brain barrier endothelial cells*
555 *from human pluripotent stem cells*. Nat Biotechnol, 2012. **30**(8): p. 783-
556 91.
- 557 39. Doster, A., et al., *Unfractionated Heparin Selectively Modulates the*
558 *Expression of CXCL8, CCL2 and CCL5 in Endometrial Carcinoma Cells*.
559 *Anticancer Res*, 2016. **36**(4): p. 1535-44.
- 560 40. Lin, X., et al., *Insights into Human Astrocyte Response to H5N1 Infection*
561 *by Microarray Analysis*. Viruses, 2015. **7**(5): p. 2618-40.
- 562
- 563
- 564
- 565

566 **Table 1. Primers used for quantification of tight junctions, receptors and**
 567 **transporters encoding genes.**

Gene	Forward primer	Reverse primer	Reference
TFRC	5'-ATG CTG ACA ATA ACA CAA-3'	5'-CCA AGT AGC CAA TCA TAA-3'	[37]
AGER	5'-CTC GAA TGG AAA CTG AAC AC-3'	5'-CTG GTA GTT AGA CTT GGT CTC-3'	[37]
LRP1	5'-GCA TCC TGA TCG AGC ACC TG-3'	5'-GCC AAT GAG GTA GCT GGT GG-3'	[37]
INSR	5'-TGT TCA TCC TCT GAT TCT CTG-3'	5'-GCT TAG ATG TTC CCA AAG TC-3'	[38]
LEPR	5'-GGA AAT CAC ACG AAA TTC AC-3'	5'-GCA CGA TAT TTA CTT TGC TC-3'	[38]
BCAM	5'-GCT TTC CTT ACC TCT AAA CAG-3'	5'-GAA GGT GAT AGA ACT GAG CG-3'	[38]
SLC6A8	5'-TGA GAG AAT GAG ATT TCT GCT TGT-3'	5'-TAG GGC TCA CAG GGA TGG-3'	[37]
SLC3A2	5'-TTG GCT CCA AGG AAG ATT-3'	5'-GAG TAA GGT CCA GAA TGA CA-3'	[37]
SLC2A1	5'-GAG ACA CTT GCC TTC TTC-3'	5'-GCT TTG TAG TTC ATA GTT CG-3'	[37]
SLC7A5	5'-TTG ACA CCA CTA AGA TGA T-3'	5'-GTA GCA ATG AGG TTC CAA-3'	[37]
SLC7A1	5'-CCT CCT GAG ACA TCT TTG-3'	5'-CTG GAA TAT GAC GGG AAG-3'	[37]
SLC16A1	5'-ACA CAA AGC CAA TAA GAC-3'	5'-ACA GAA TCC AAC ATA GGT A- 3'	[37]
ABCB1	5'-GCC TGG CAG CTG GAA GAC AAA TAC ACA AAA TT-3'	5'-CAG ACA GCA GCT GAC AGT CCA AGA ACA GGA CT-3'	[37]
ABCG2	5'-TGG CTG TCA TGG CTT CAG TA-3'	5'-GCC ACG TGA TTC TTC CAC AA-3'	[37]
ABCC1	5'-ACC AAG ACG TAT CAG GTG GCC- 3'	5'-CTG TCT GGG CAT CCA GGA T- 3'	[37]
ABCC2	5'-CCA ATC TAC TCT CAC TTC AGC GAG A-3'	5'-AGA TTC CAG CTC AGG TCG GTA CC-3'	[37]
ABCC4	5'-AAG TGA ACA ACC TCC AGT TCC A- 3'	5'-CCG GAG CTT TCA GAA TTG AC-3'	[37]

Gene	Forward primer	Reverse primer	Reference
ABCC5	5'-AGT GGC ACT GTC AGA TCA AAT T-3'	5'-TTG TTC TCT GCA GCA GCA AAC-3'	[37]
STRA6	5'-TTT GGA ATC GTG CTC TCC G-3'	5'-AAG GTG AGT AAG CAG GAC AAG-3'	[38]
SLC38A5	5'-TGT CAG TGT TCA ACC TCA G-3'	5'-GTG GAT GGA GTA GGA CGA-3'	[38]
SLC1A1	5'-GTT ATT CTA GGT ATT GTG CTG G-3'	5'-CTG ATG AGA TCT AAC ATG GC-3'	[38]
PLVAP	5'-CAA TGC AGA GAT CAA TTC AAG G-3'	5'-ACG CTT TCC TTA TCC TTA GTG-3'	[38]
CXCL8	5'-TCT TGG CAG CCT TCC TGA TT-3'	5'-TTA GCA CTC CTT GGC AAA ACT G-3'	[39]
CXCL10	5'-TGG CAT TCA AGG AGT ACC TCT C-3'	5'-CTT GAT GGC CTT CGA TTC TG-3'	[40]
GAPDH	5'-AGC CAC ATC GCT CAG ACA CC-3'	5'-GTA CTC AGC GCC AGC ATC G-3'	[37]

568

569

570 FIGURE LEGENDS

571 **Fig. 1. The presence of SK-N-SH cells under hCMEC/D3 BBB-forming cells**
572 **does not affect the BBB properties.** hCMEC/D3 were cultivated on
573 Transwell® inserts. Five days after seeding, SK-N-SH (SK) cells were cultivated
574 or not in wells under the Transwell® inserts (white and black bars respectively).
575 **A)** Twenty-four hours after adding the SK-N-SH cells (+) or not (-), BBB
576 permeability to LY was measured. **B)** and **C)** hCMEC/D3 BBB-forming cells total
577 RNA was extracted and receptors (B) and transporters (C) typical of the BBB-
578 encoding genes were quantified by RT followed by qPCR as described in
579 Material and Methods. Graphs show the results from two independent
580 experiments performed by duplicates.

581 **Fig. 2. JEV RP9 is more replicative than JEV SA14-14-2 in SK-N-SH**
582 **neuroblastoma cells.** SK-N-SH cells were infected at MOI 0.1 for 24 or 48h by
583 the indicated JEV strain. **A)** The infected cells were analyzed at the indicated
584 times post-infection by immunofluorescence staining for the presence of the
585 NS5 protein (in green). The images were taken at a x200 magnification, the cell
586 nuclei were stained by DAPI (in blue). **B)** Supernatants of SK-N-SH cells
587 infected by JEV RP9 (black bar) or JEV SA14-14-2 (white bar) were titrated in
588 Vero cells. The arithmetic means \pm standard deviation of three independent
589 experiments performed in triplicate is shown. Asterisks indicate a significant
590 difference between RP9 and SA14-14-2 in each one of the times post-infection
591 evaluated (**, $P < 0.01$, ***, $P < 0.001$).

592 **Fig. 3. Infection of hCMEC/D3 cells by JEV strains.** hCMEC/D3 were
593 cultured on coverslips for either 6 days (**A**) or 1 day (**B**), so that they form or not
594 a BBB respectively. Cells were then inoculated with the indicated JEV strain at
595 MOI=0.1 and analyzed at 24 and 48 hpi by immunofluorescence staining for the
596 presence of the NS5 protein (in green). The images were taken at a x200
597 magnification, the cells nuclei are stained by DAPI (in blue). **C)** Supernatants
598 from hCMEC/D3 cells that do not form a BBB and infected by JEV RP9 (black
599 bar) or JEV SA14-14-2 (white bar) were collected at 24 and 48 hours post-
600 infection and their viral titer was determined as described in Material and
601 Methods. The arithmetic means \pm standard deviation of three independent
602 experiments performed by triplicate is shown. Asterisks indicate a significant
603 difference between RP9 and SA14-14-2 in each one of the times post-infection
604 evaluated (**, $P < 0.01$, ***, $P < 0.001$).

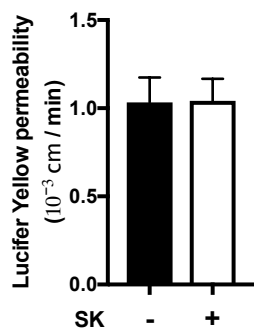
605 **Fig. 4. JEV RP9 and JEV SA14-14-2 may cross the *in cellulo* BBB model**
606 **without disrupting it. A)** hCMEC/D3 cells were cultivated on Transwell®
607 inserts. Five days after seeding, SK-N-SH cells were added to the wells under
608 the Transwell® insert. 24h later JEV RP9 or SA-14-14-2 was added either at
609 MOI=1 or =10 to the BBB as indicated. Permeability to Lucifer Yellow was
610 assayed in the hCMEC/D3 cells 6 h post-addition as described in Material and
611 Methods. **B)** *In cellulo* BBBs were generated as indicated above and either JEV
612 strain was added at MOI=1 or =10. After 6 h, total RNA was extracted from JEV
613 BBB-crossing samples under the inserts and the number of JEV RNA copies
614 was determined by RT-qPCR as described in Material and Methods. **C)** Either
615 JEV RP9 (black bars) or SA14-14-2 (white bars) BBB-crossing samples were
616 collected after 6 h post-addition and their viral titer was determined as described
617 in Material and Methods. The arithmetic means \pm standard deviation of at least
618 two independent experiments performed by triplicate is shown. Asterisks
619 indicate a significant difference between the RP9 and SA14-14-2 titers in each
620 one of the MOIs evaluated in the BBB-crossing experiments (****, $P < 0.0001$).

621 **Fig. 5. The specific infectivity of JEV RP9 is decreased after BBB-**
622 **crossing. A)** Both the number of viral RNA copies and the infectious titers for
623 either JEV RP9 or JEV SA14-14-2 stocks used for the JEV BBB-crossing
624 experiments were determined as described in Material and Methods. The
625 specific infectivity of both stocks was calculated by dividing the viral RNA copies
626 number/ml by the FFU/ml of each viral stocks. B) The specific infectivity of the
627 JEV RP9 and SA14-14-2 BBB-crossing samples was calculated as indicated
628 above using the data from Fig. 4B and 4C. The arithmetic means \pm standard
629 deviation of at least two independent experiments performed by triplicate is

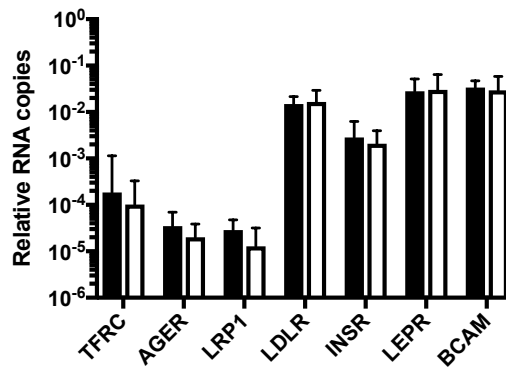
630 shown. Asterisks indicate a significant difference between the specific infectivity
631 of RP9 and SA14-14-2 in each one of the MOIs evaluated in the BBB-crossing
632 experiments (**, $P < 0.01$; ****, $P < 0.0001$).

Fig. 1

A)



B)



C)

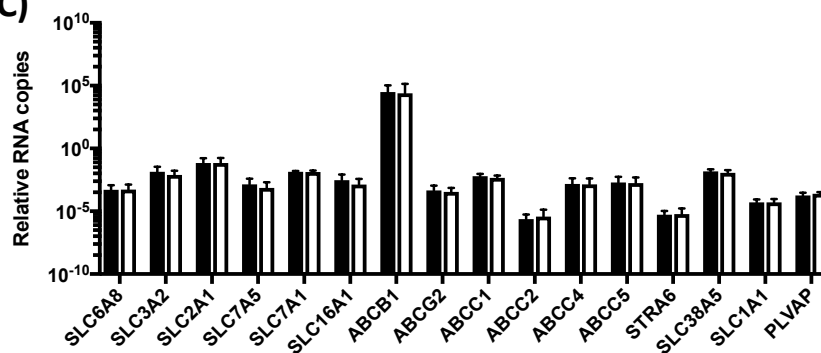


Fig. 2

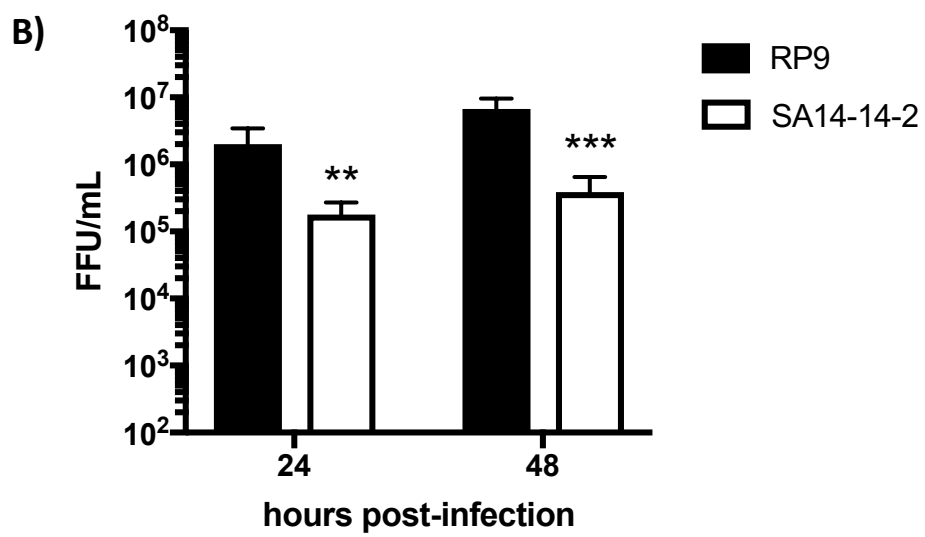
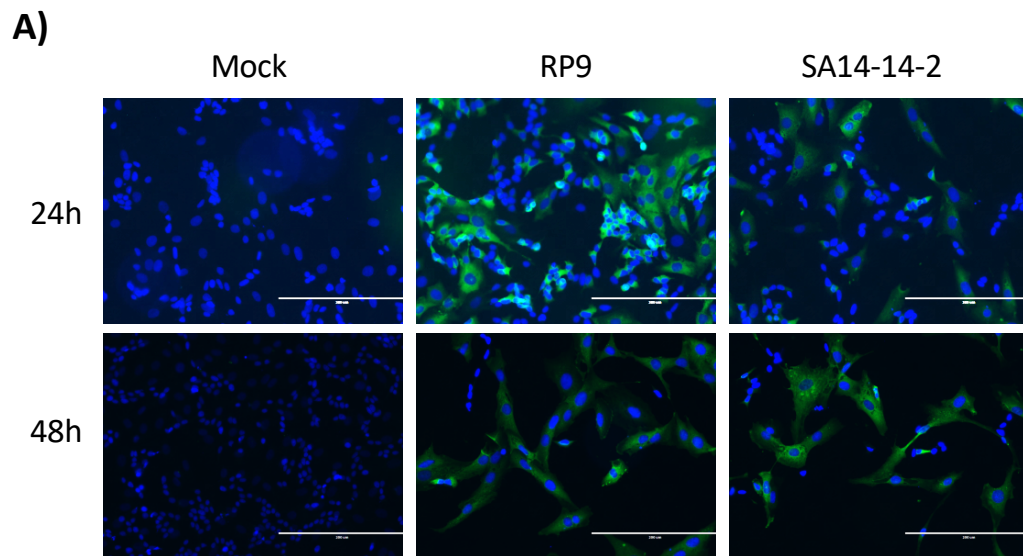


Fig. 3

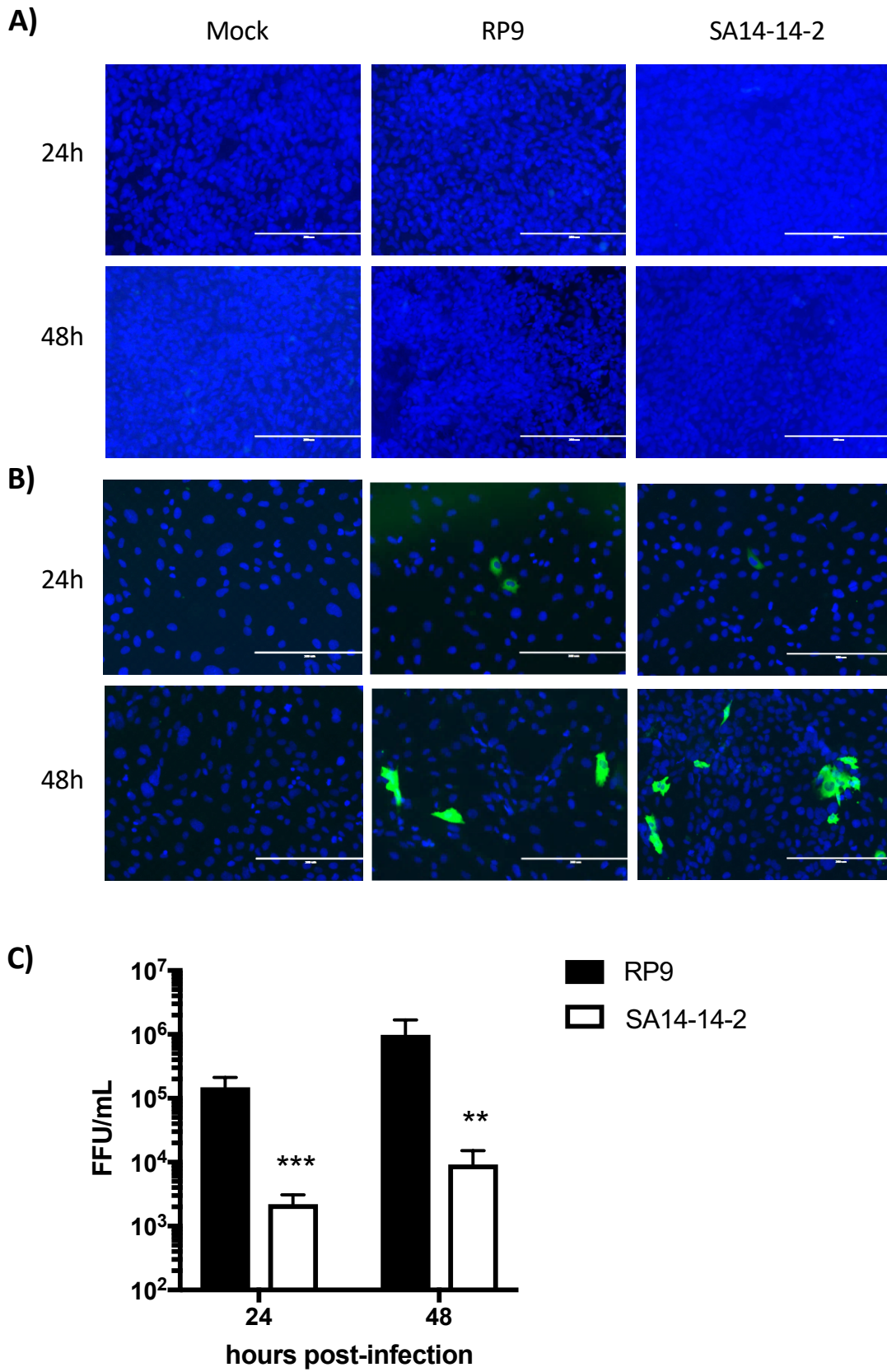


Fig. 4

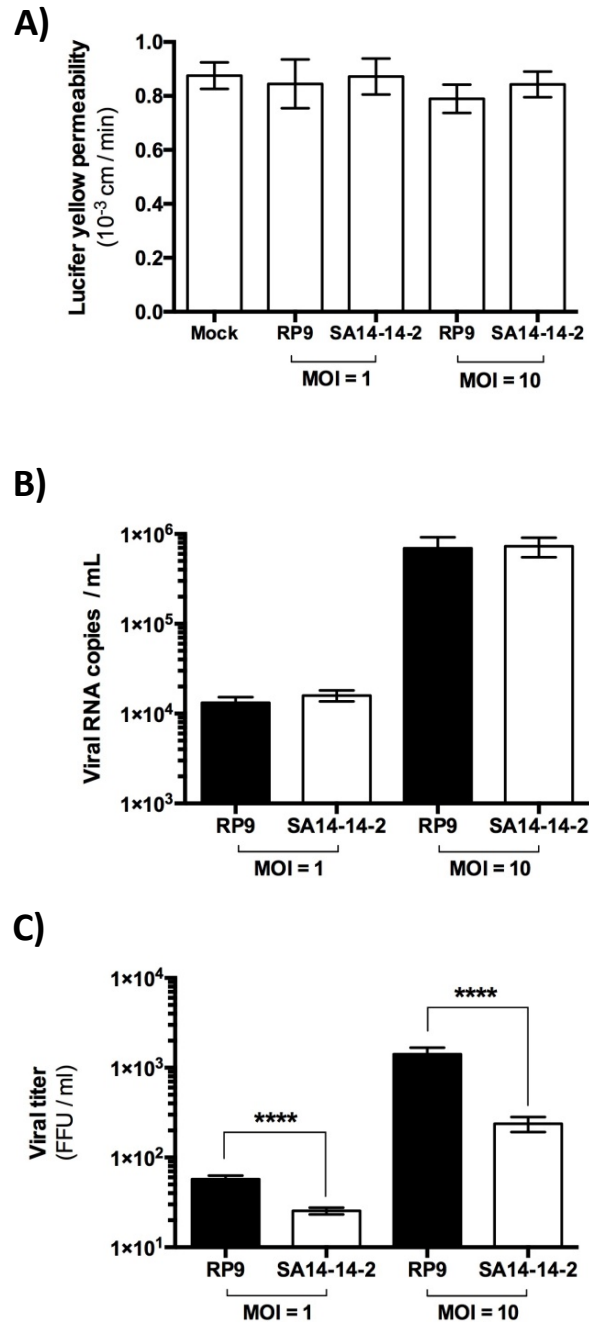
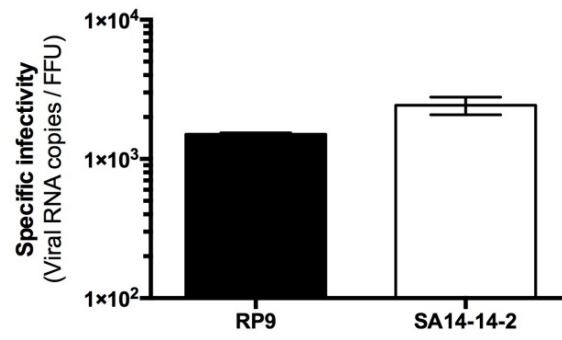


Fig. 5

A)



B)

